STM JOURNALS

Journal of
Polymer & Composites

ISSN: 2321-2810 (Online)
ISSN: 2321-8525 (Print)
Volume 12, Special Issue 4, 2024
DOI (Journal): 10.37591/JoPC

https://journals.stmjournals.com/JOPC/

Research JoPC

Synthesis of Biofuel from Castor Oil Using Novel Catalysts

Muthuluru Rajesh[1,*], V.L. Mangesh[2], G. Murali[3], R. Jai Ganesh[4]

Abstract

An essential step in improving biofuels, especially those made from biomass, is hydrodeoxygenation (HDO). HDO's primary goal is to eliminate oxygen atoms from the biofuel feedstock in the form of water, which enhances the fuel's energy density, stability, and compatibility with current fuel.This study uses a large surface area catalyst to investigate the hydrodeoxygenation (HDOx) activity of non-edible oils. In addition to other supports including H-USY and MCM-41, large surface area catalyst Co/Pt-HZSM-5 was used to comprehensively analyze and compare the HDOx activity. Reverse order impregnation was used to construct Co-Pt bimetal supported over mesoporous HZSM-5, which facilitated HDOx of non-edible oils. Methods including BET and TPD were employed to analyze and describe the catalysts that were generated. The HDOx roles for the preparation of long-chain, saturated hydrocarbons in a fixed bed high-pressure stainless- steel reactor operating between 290°C and 370°C and a hydrogen pressure of 10–50 bar were significantly impacted by the synthesized catalysts. High amounts of H2 consumption, acidity, and texture were found in Co/Pt-HZSM-5. The relationship between structure and activity was examined and distribution of products were overviewed. Even if there are still issues with catalyst deactivation and hydrogen consumption, this study will support continued research and technological developments to improve the viability and efficiency of HDO in the manufacture of biofuels.

Keywords: Biofuels; hydrodeoxygenation; castor oil; hydrocarbons; non- edible oil

INTRODUCTION

The necessity for less pollution and a reduced reliance on fossil fuels for transportation in the future has made global biofuel research imperative. Biofuel made from biomass has more environmental benefits and is sustainable and renewable. The use of fossil fuels is decreased by the method's effectiveness and environmental friendliness. In order to produce ultra-clean biofuel energy using various catalytic hydrotreatment processes, numerous good studies have been carried out [1-3]. Special attention has been paid to hydrodeoxygenation (HDOx), which is a sustainable and renewable chemical and biofuel production process using lignocellulosic biomass [4]. The early bio-based oil extracts have drawbacks, including high oxygen content that sets off the oil's tendency to polymerize during transit and storage, as well as being caustic and incompatible with fossil fuels. They are exceedingly viscous, corrosive, and have a low heating value once more [5]. To comply with particular cations for gasoline, this necessitates improving the oil extracts. Globally, we have an ongrowing demand for renewable and green fuels, and regulations are being put in place to limit the

***Author for Correspondence**
Muthuluru Rajesh

[1]Research Scholar, Départements of Mechanical Engineering, Koneru Lakshmaiah Education Foundation, Green Fields, Vaddeswram, Andhra Pradesh, India.
[2]Professor, Department of Mechanical Engineering, Koneru Lakshmaiah Education Foundation, Green Fields, Vaddeswram, Andhra Pradesh, India.
[3]Professor, Department of Mechanical Engineering, Koneru Lakshmaiah Education Foundation, Green Fields, Vaddeswram, Andhra Pradesh, India.
[4]Research Associate, Department of Mechanical Engineering, Koneru Lakshmaiah Education Foundation, Green Fields, Vaddeswram, Andhra Pradesh, India.

Received Date: April 06, 2024
Accepted Date: July 05, 2024
Published Date: July 18, 2024

Citation: Muthuluru Rajesh, V.L. Mangesh, G. Murali, R. Jai Ganesh. Synthesis of biofuel from castor oil using novel catalysts. Journal of Polymer & Composites. 2024; 12(Special Issue 4): S226–S237.

damaging impacts of industry on the environment [6-8]. The HDOx reaction will meet the needs of industry for both HDOx and a substitute for conventional fossil oils and are free from contaminants. [9,10] Prior research has demonstrated the use of a range of catalysts to convert non-food oils, including algal oil, palm oil, castor oil, and long fatty acid chains, into hydrocarbon fuels [11,12]. Because of their special qualities, some class of mesoporous materials for example, zeolites and silica descendants have attracted noteworthy interest from a variety of fields [13]. These materials are very desired because of their enormous pore volume, modifiable dispersion in their pore sizes with broader surface area. Furthermore, mesoporous materials have shown to be successful in cleaning up the environment. Often used on zeolite supports, noble metals have a yield in HDOx that is much higher than that of traditional catalysts. Larger industrial applications are, however, constrained by higher costs [14]. Mesoporous materials like zeolites and derivatives of silica have a lot of potential in the energy sector for a variety of uses [15-20]. Zeolites play remarkable role in catalysis in many endothermic processes like isomerization and hydrocarbon cracking. A major factor influencing the guaiacol HDOx is the shape selectivity of the zeolite material [21].

Excellent activity has been reported by noble metals like palladium, platinum and ruthenium in the bio feedstock hydrotreatment to turnover alternate fuel [22-25]. High-pressure reactions are necessary for noble metal catalysts to function, and also their high price and limited supply prohibit their widespread application [26,27]. Consequently, the focus has been on trying to employ less precious, affordable metals for performing catalysis with comparable effectiveness. Some d-block metals such as Nickel, Cobalt, and Molybdenum are employed to replace precious metals as efficient catalysts and promoters of the HDOx process. Bimetal combinations supported over conventional Al_2O_3 catalysts were shown to be the most effective catalyst for HDOx of castor oil, algal oil, palm oil, and long fatty acid chains employed in the production of low emission combustibles [28-32].

There are various drawbacks to supports composed of TiO_2, ZrO_2, CeO_2, and $Al2O_3$, including reduced surface coverage, poor active metal dispersion over available sites, and detatchment of metals by chemical dissolution. Zeolites supported over d-block metal catalysts with enhanced catalyst traits, such as minimal deactivation, attracted increasing attention [33,34]. Improving dispersion area of metals rocket up the catalyst's effectiveness and prolongs the expected lifespan of the catalyst. The mean dimension of the particles within the active element is a crucial factor in the reaction.. In the study here, Co–Pt bimetal catalysts were used to zeolites for the HDOx of castor oil, as zeolites are favorable for HDOx due to all these aspects [35,36]. Once more, noble metals like Pt are pricey, but their longer catalyst lives allow for higher conversion efficiencies. The current investigation centers on a heterogeneous mixed metal catalyst devoid of sulfide compounds, supported by substrates exhibiting both neutral and acidic properties. The preferential selectivity and HDOx conversion of castor oil depend on this catalyst [37]. HDOx has shown promising results when combined with Co thanks to the low cost and widespread availability of natural zeolites. The HDOx method favours crude bio-oil products because they produce hydrocarbons, making them an inedible fuel. Similar to popular fossil fuels like diesel, kerosene, light naphtha, and jet fuel, these hydrocarbons have the same energy density. The active metal species in HDOx processes have recently been dispersed using various mesoporous materials such like MCM-41, SBA-15, KIT-6 etc. [38-43].

In the current work, we used the catalyst Co/Pt/HZSM-5 having high surface coverage to convert non-edible oils. We carried out a thorough analysis and comparison of the HDOx activity. comprehensively examined and contrasted the HDOx activity utilizing the ample coverage catalyst Co/Pt/HZSM-5 and additional mesoporous structures which include MCM-41 and H-USY. The experiments were conducted at various temperatures and with high pressure conditions between 15 and 30 bar conducted in a fixed bed high-pressure stainless steel reactor. The link among structural activity with the catalyst has been made clear. An observation was noted indicating that the diverse acidic pockets and texture attributes of HZSM-5 mesoporous base supports have an impact on the activity of HDOx.

EXPERIMENTAL METHODS

Synthesis of Mesoporous HZSM-5 Zeolite

Modified versions of previously described procedures are the ones outlined below [44]. HZSM-5 zeolite mesoporous materials were sourced from a gel matrix using silane coupling agent $C_{26}H_{58}NO_3SiCl$ (DTSACl), a 75% methanol solution along with molecular templating agent $(CH_3CH_2CH_2)_4N(Br)$ (TPABr) as a pattern. To create solution A, the following steps were taken to synthesize a conforming gel matrix: 0.7 g of metakaolin, 0.6 g of sodium hydroxide powder and 1.8 g of $(CH_3CH_2CH_2)_4N(Br)$ were added to 52 g of double distilled water and vigorously stirred for about half an hour at ambient temperature conditions, until our resulting mixture was homogenous. A homogenous mixture of 4.35 g of $C_8H_{20}O_4Si$ (Tetraethyl orthosilicate - TEOS) and after two hours of continuous stirring, 0.65 g of Octyl decyl dimethyl ammonium chloride (ODDAC) was introduced into the ultimate blend of A, resulting in the formation of a gel. After that, the mixture was placed inside a pre-scrubbed stainless -steel autoclave and was maintained at 180 °C for about a day. The resulting substance was properly cleaned, allowed to be dried throughout the night at 100 °C, and then the temperature was adjusted to 550 °C for six hours while exposed to air, with a 5°C per minute heating rate.

Synthesis of Mesoporous MCM-41 Zeolite

Starting with 45 mL of double distilled water and mixing it with 4.8 grams of $C_{19}H_{42}BrN$ (Cetyl trimethyl ammonium bromide - CTAB). 0.62 g of $Al(NO_3)_3$ were added, and the mixture is stirred vigorously nearly for an hour (60 min). After adding 10-12 mL of 34 wt% NH_4OH and 60 mL of HPLC grade rectified spirit, the mixture was vigorously stirred for 30 minutes. After that, 7.23 g of $C_8H_{20}O_4Si$ (Tetraethyl orthosilicate - TEOS) were added to the mixture once more, and is stirred continuously for about two days (48 h). The latter was continuously refluxed at ambient temperature for two days (48 h). The resultant was allowed to dry in hot air oven at 120°C for 48 h before being filtered. In the end, the sample was heated for five hours to 550°C [45].

Synthesis of Mesoporous H-USY Zeolite

Stirred for about 45 min, 0.867 g of $Al_2(SO_4)_3.18H_2O$ (Aluminum sulphate octadecahydrate), 0.652 g of powdered NaOH, and 6.1 g of 40% $C_8H_{21}NO$ (Tetra ethyl ammonium hydroxide – TEAOH) were added and stirred until the resultant become semi-transparent. Then the resulting contents were stirred approximately an additional 60 min and then 3.25 g of silica powder was introduced. The outcome was a viscous gel mass that was air dried at 65°C. After that, the dried contents were coarsely pulverized and put into a 4 mL PTFE (polytetrafluoroethylene) container, and is placed within a 20 mL PTFE liner. Without disturbing corresponding dry gel within the internal PTFE container, nearly 0.5 mL of double distilled water was added to the liner bottom. Then the steel 20 mL reactor held the electrified liner assembly. After two to three days of heating the oven to 150°C, the reaction was quenched. After being transformed, the gel was cleaned and filtered before being dried. For six hours, the template was calcinated at the temperature of 550°C the gradient increasing at the rate of 2°C per minute. Si/Al ratios from the calcinated sample's elemental analysis were quite proximate to the abstract values stated in the research articles. The solution of Colloidal particles were centrifuged three times at 20,000 rpm for at least 40-50 minutes to eliminate the particulates. At last, the end product was dried for 5 hours at 550°C [46].

Co Metals Impregnation on Solid Support

In this study, the desired mesoporous zeolites (HZSM-5, MCM-41 and H-USY) were annexed to 1% cobalt by embedding with aqueous $Co(NO_3)_2.6H_2O$ (cobalt(II) Nitrate hexahydrate) solution, dried in hot air oven them for 6 h at 110°C, and then calcinating them for 2 h at 550°C in an air flow.

Platinum Metals Impregnation on Supports

The catalysts were treated with an aqueous solution of H_2PtCl_6 to impregnate them with platinum (0.5%). Afterwards, they underwent dehydration at 120°C for a duration of 6 h followed by calcination at 450°C under airflow for 2 h. The HDOx catalyst was introduced into the reactor while maintaining the platinum in its reduced state at a temperature of 200°C under a H_2 flow.

Catalytic Activities

A vapor phase high pressure fixed-bed reactor has been used to measure the catalyst's HDOx activity. The feed used in this study consisted of high purity hydrogen and castor oil which were dissolved in decahydronaphthalene. The display screen monitored the pressure and temperature. In the bed, inert silica wool and glass beads were positioned alongside 3.25 g of catalyst particles, which were utilized for support and measured 380 mm in length with a diameter of 15 mm. The liquid feed is vaporized in order to properly mix it with the catalyst before it reaches the catalyst bed. Variables such as temperatures ranging from 290 to 370°C, pressure set at 30 bar, and the weight hourly space velocity (WHSV) were influential factors in the hydrodeoxygenation (HDOx) process of castor oil. Upon the conclusion of the reaction, both the liquid and gaseous components were gathered and collected for further analysis. The Shimadzu-GC-17A gas chromatograph instrument with DB-5 column was used to analyze the product after it was collected at different times. The concentrations measured at the start and end of the process (in moles) as determined by gas chromatography were employed in computing the conversion rate of castor oil.

Catalyst Characterization

The synthesized catalysts underwent characterization employing an array of physical and chemical methodologies, including temperature programmed desorption (TPD) and N_2 physisorption investigations. The N_2 sorption isotherms at the temperature of liquid nitrogen were measured using the QUADRASORB SI automated analyzer, which was employed for this purpose. Before analysis, a 30 mg sample was subjected to degassing with a flow of nitrogen for a duration of 4 h at a temperature of 300°C. The specific surface dimensions of both the support and the catalyst were determined using the BET method. The pore volume (Vp) was calculated using N_2 adsorption at 1 bar relative pressure, while a graph showing pore size distributions from the desorption isotherms was created using the BJH method. Temperature-programmed desorption experiments were conducted utilizing the Micromeritics Chemisorb 2750 TPD instrument. These tests employed gas mixtures consisting of 10% ammonia and 90% helium, as well as 5% hydrogen and 95% argon, respectively, for their respective analyses. Before analysis, a sample weighing 30 mg underwent degassing with a flow of N_2 gas for a duration of 3 h at a temperature of 200°C.

RESULTS AND DISCUSSION

BET analysis

Let us for simplicity from now on abbreviate Co/Pt/HZSM-5 as MZC-A, Co/Pt/MCM-41 as MZC-B and Co/Pt/H-USY as MZC-C. Fig.1 illustrates the N_2 adsorption and desorption isotherms for the prepared MZC-A, MZC-B and MZC-C modified zeolite catalysts. The observed isotherm in all instances corresponds to a type IV classification. The creation of additional mesopores [47] in our modified zeolites led to the generation of a wider hysteresis loop, spanning from $P/P_0 = 0.46$ to $P/P_0 = 1$, as evidenced in this investigation. Table 1 presents the area of surfaces and volume of pores for the modified catalysts MZC-A, MZC-B, and MZC-C prepared based on experimental findings, showcasing variations across different zeolite samples. Table 1 exhibits the area of surfaces and volume of pores derived from BET analysis for the MZC-A, MZC-B, and MZC-C catalysts, showcasing figures of 395.21 $m^2\ g^{-1}$, 0.459 $cm^3\ g^{-1}$, 358.87 $m^2\ g^{-1}$, 0.394 $cm^3\ g^{-1}$, 360.15 $m^2\ g^{-1}$, and 0.331 $cm^3\ g^{-1}$, respectively. Additionally, it provides macrospore volumes of 0.07 $cm^3\ g^{-1}$, 0.08 $cm^3\ g^{-1}$, and 0.33 $cm^3\ g^{-1}$ for MZC-A, MZC-B, and MZC-C, respectively. The macrosporal volumes across the three distinct catalysts are fundamentally identical. These findings indicate the preservation of microporosity alongside the generation of surplus mesoporosity.. Reactant molecules diffuse more strongly in MZC-A because of its greater mesoporosity compared to MZC-B, and MZC-C. Relative to MZC-C, the MZC-A modified zeolite exhibits a wider surface dimensions and volume of pores. The results indicated that incorporating the non-ionic surfactants alongside the synthesis of the active catalyst facilitated the development of extra mesoporosity in MZC-B samples without disturbing the catalyst's microporosity. [48].

NH_3 - TPD Analysis

The acidic properties of the zeolite catalysts MZC-A, MZC-B, and MZC-C were assessed through the NH_3 - TPD technique. The corresponding TPD results of the MZC-A, MZC-B, and MZC-C zeolite catalysts were displayed in Fig. 2 [49]. The two desorption peaks for MZC-A, MZC-B, and MZC-C zeolite catalysts can be seen, as indicated in Fig. 2, with low temperature (L.T) peak at about 200°C and high temperature (H.T) peak at 400°C. The L.T peak originates from NH3 adsorption at weak acidic sites, whereas the H.T peak is associated with desorption of NH_3 from strongly acidic sites (Bronsted and Lewis acid sites). Comparable ammonium desorption profiles are found in zeolites composed of MZC-A, MZC-B, and MZC-C. The peak intensities observed in all zeolite catalysts are notably higher when contrasted with those of MZC-A, MZC-B, and MZC-C [50]. The minimal Co/Pt concentration within the zeolite framework contributes to the diminished acidity of MZC-C. Meanwhile, the reduced acid strength of MZC-B zeolite is attributed to the presence of amorphous aluminum silicate within the macrospore walls.

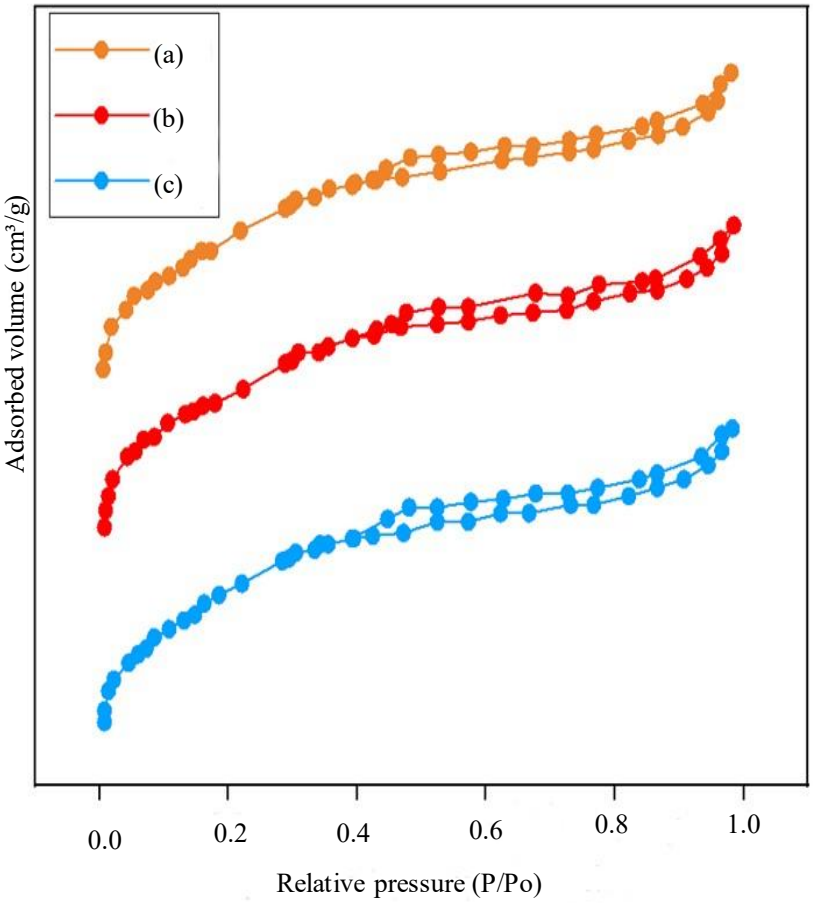

Figure 1. Nitrogen adsorption and desorption studies of (a) MZC-A, (b) MZC-B and (c) MZC-C

Table1. BET surface areas and pore volumes analysis of the modified zeolite catalysts.

Catalyst	SA_{BET}[e] (m^2g^{-1})	Pore volume[f] (cm^3g^{-1})	D_p^g (mm)	Acidity[g] (mmol g^{-1})[2]	L.T peak[g]	H.T peak[g]	Si/Al ratio[h]	Co[h] (wt%)	Pt[h] (wt%)
MZC-A	395.21	0.459	3.15	1.59	0.97	0.62	49.3	1.15	0.52
MZC-B	358.87	0.394	4.07	1.45	0.93	0.55	49.24	0.99	0.55
MZC-C	360.15	0.331	3.65	1.42	0.85	0.53	48.72	1.23	0.48

[e]Determined from the t-plot method, [f]Vmesoporosity = Vtotal – Vmicroporosity, [g]Total acidity derived by TPDA method, L.T = low temperature, H.T = high temperature, [h]Chemical composition of the catalysts, determined using ICP-OES.

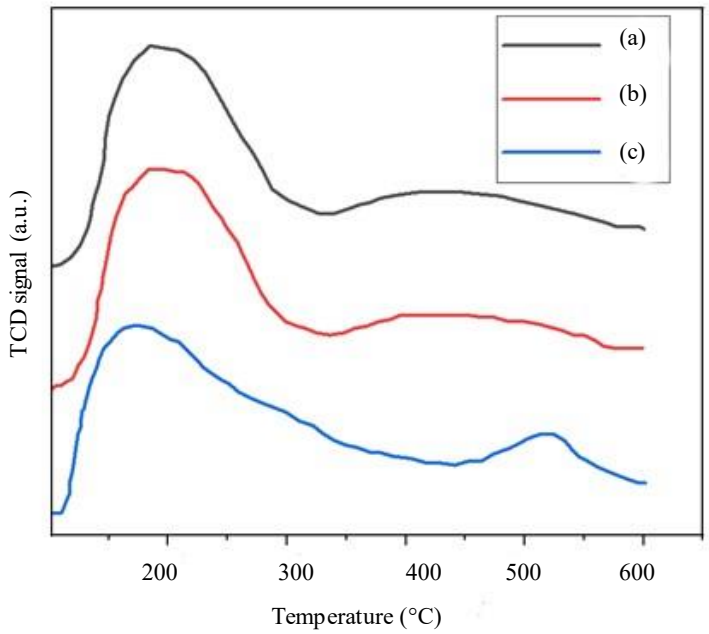

Figure 2. Temperature-programmed desorption analysis of (a) MZC-A, (b) MZC-B and (c) MZC-C catalysts.

CATALYST PERFORMANCE ANALYSIS

Influence of Supports

The findings of this investigation into the synthesis and assessment of Co–Pt catalysts utilizing diverse aluminum silicate supports, such as MZC-A, MZC-B, and MZC-C, for castor oil hydrodeoxygenation (HDOx), are displayed in Fig.3. Each catalyst underwent testing in uniform conditions, maintaining a 350 °C steady temperature with a pressure of 30 bar throughout. The existence of weak acid sites was identified to be more pronounced within the MZC-A catalyst which is one of the factors that contribute to the catalyst's performance. The MZC-A catalyst performs better than the other supported catalysts, with its surface coverage, pore volume and pore dimensions all contributing to the efficacy of the catalyst. As a result of deficiency of the active pockets in its surface, the MZC-B modified zeolite exhibited the lowest activity. In contrast to the other supported catalysts, the Co–Pt metals incorporated within HZSM-5 (MZC-A) exhibit superior conversion efficiency. The catalysts exhibited their highest catalytic activity in the following sequence: MZC-A demonstrated the greatest efficacy, followed by MZC-B, and then MZC-C.

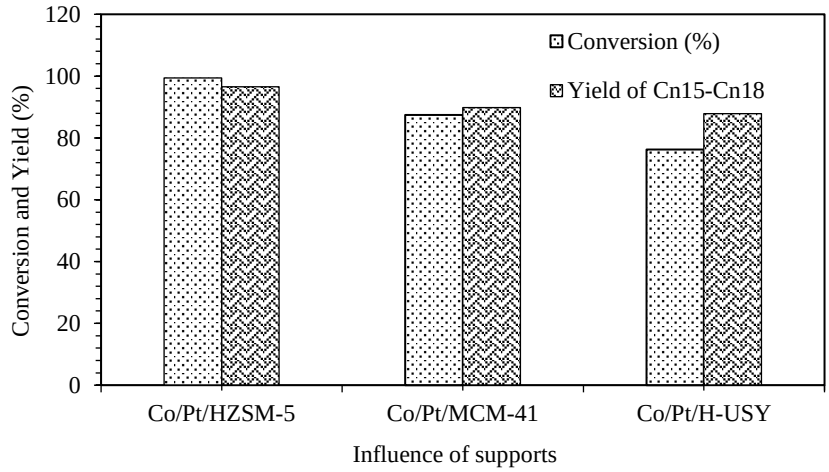

Figure 3. Influence of supports at 30 bar constant pressure and 350°C reaction temperature, precursor: 7% castor oil in decahydronaphthalene, weight hourly space velocity = 1 h^{-1}, Time elapsed: 8 h; H_2

Castor Oil: Molecular Weight Profile

Molecular weight (M.W) distribution of castor oil was assessed using polystyrene standards and gel permeation chromatography (GPC). In the castor oil, M.W was distributed rather widely. 8.5% castor oil decahydronaphthalene, 1 h^{-1} weight hourly space velocity, 10 h, 50 mL/min hydrogen flow, 320°C temperature, and 30 bar constant H_2 pressure are the reaction parameters. The findings of the Gel Permeation Chromatography analysis revealed the presence of three discernible peaks initially, characterized by average molecular weights of 1765, 877, and 457, respectively, along with retention times of 8.2, 8.5, and 9.1 minutes, respectively. Reaction times (RT) of 8.3, 8.5, and 9.3 min were found after catalytic formation in terms of M.W. Subsequently, these measurements were modified to reflect durations of 8.6 and 9.7 min, corresponding to an average molecular weight of 806 and 97, respectively. It was deduced that this unequivocally demonstrates the migration of GPC peaks towards the lower molecular weight spectrum in response to variations in both temperature and pressure.

For convenience, let us now abbreviate carbon number to be Cn. It is indicated that a decrease in intensity is due to further depolymerization. Therefore, it can be inferred that the main long chains were converted into hydrocarbons with carbon chain lengths ranging from Cn_{15} to Cn_{18}. At 350°C, the retention time continued to decrease, with average M.W of 485 and 180 observed, respectively. Similar outcomes were obtained when converting all kinds of long chains into Cn_{15}–Cn_{18} hydrocarbons. The GC analysis's results also revealed the same kind of outcomes. The temperature was raised to 365 °C, but the retention times were still 8.7 and 9.2 section minutes, with average M.W = 390 and 180, respectively. Nevertheless, increased hydrocracking and the accumulation of deposits on the active pocket surfaces resulted in the production of Cn_1–Cn_{14} hydrocarbons and subsequent coke formation. Consequently, it might be induced by the compounds breaking down into smaller hydrocarbons, thereby obstructing the acidic regions on the surface's outermost layer. Gel permeation chromatography results showed that the optimal temperature for greater conversion, specifically for (Cn_{15}-Cn_{18} hydrocarbons), was 350 °C [51].

Influence of Temperature

By using Co-Pt metals incorporated on mesoporous MZC-A zeolite, Figure.4 shows how temperature affects the hydrodeoxygenation (HDOx) of castor oil. The procedure comprised turned the oil into biofuel at temperatures between 290 and 370°C with a supply of 30 bar constant H_2 pressure. The predilection for carbon chain compounds of Cn_{15}, Cn_{16}, Cn_{17}, and Cn_{18} was evident in the transformation of liquid products, achieving percentages of 74.6% and 87.4% at temperatures of 300 °C and 325 °C, respectively. At temperatures of 300°C and 325 °C, the respective proportions of these products were 23.6%, 31.47%, 15.33%, and 23.44%, and 18.7%, 27.1%, 16.4%, and 26.5%. Lower alkanes (Cn_1–Cn_4 at 3%), as byproducts, were produced at lower concentrations at this higher temperature. Table 2 shows that more cracking products, such as Cn_5–Cn_{14} and >Cn_4, formed at higher temperatures as a result of coking, or carbon deposition, on the catalyst, which blocked acidic sites. After reaching 375°C, the HDOx of castor seed oil showed selectivity towards the Cn_{15}–Cn_{16}/Cn_{17}–Cn_{18} ratio of up to 80%. The ratio of Cn_{15}–Cn_{16}/Cn_{17}–Cn_{18} rose noticeably between 300 and 350°C. A decline in the ratio between Cn_{15}–Cn_{16} and Cn_{17}–Cn_{18}, potentially attributable to coke formation or carbon accumulation on the catalyst, coincided with this rise in selectivity. Referring to the data provided in Table 2, it was concluded that the optimal reaction parameters were 30 bar pressure and 350°C temperature [52].

Effect of WHSV

A Co/Pt/HZSM-5 (MZC-A) catalyst was used to hydrodeoxygenate (HDOx) castor oil under a 350°C, 30 bar constant and pressure respectively. The study analyzed how varying the weight hourly space velocity (WHSV) affected the outcome of this process. To understand how the process is affected, the range of WHSV from 0.5 to 2.5 h^{-1} was explored. Selectivity was found to decrease to an ideal level as space velocity increased. Thus, at 0.5 h, the conversion was 100% ; at 2.5 h, it was 66%. The percentage of carbon chains with Cn_{14}, Cn_{15}, Cn_{16}, Cn_{17}, and Cn_{18} that exhibited selectivity decreased from 21.4%, 25.6%, 17.3%, and 31.7 percent, respectively, to 23.6%, 28.4%, 19.4%, and 16.6%. At a

WHSV value of 1 h^{-1}, the highest levels of conversion and selectivity were achieved. However, when the WHSV was increased to 2.0 h^{-1}, as there were no surface molecule interactions, the selectivity of the carbon chains in Cn_{14}, Cn_{15}, Cn_{16}, Cn_{17}, and Cn_{18} decreased. Specifically, there was a significant decline in selectivity for Cn_{17} and Cn_{18}, leading to an increased selectivity for Cn_{15} and Cn_{16} on their own. Selectivity in conversion of the carbon numbers at particular WHSV's are depicted in Table 3.

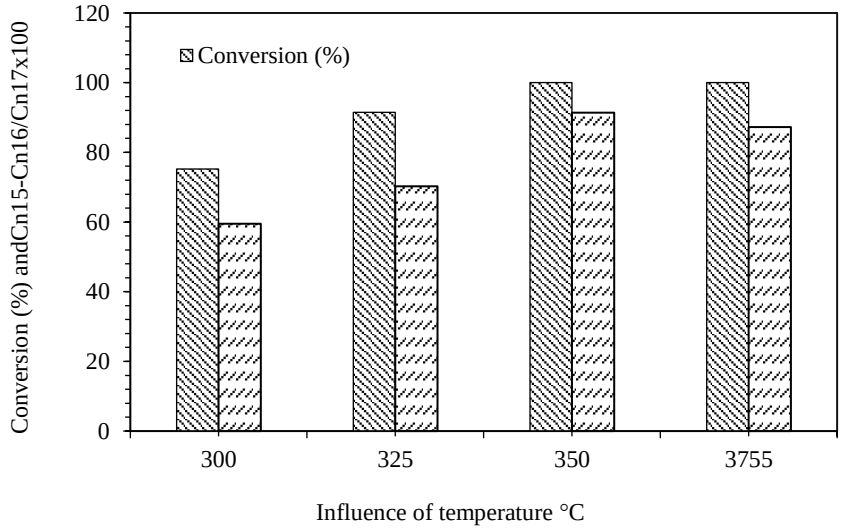

Figure 4. Influence of temperature, HDOx activity in castor oil for conversion and $Cn_{15\text{-}16}/Cn_{17\text{-}18}$ ratio at constant pressure of 30 bar, WHSV = 1 h^{-1}, time elapsed: 10 h; rate of H_2 flow = 3600 mL h^{-1}.

Table 2. Influence of temperature, HDOx of castor oil for $Cn_{15\text{-}16}/Cn_{17\text{-}18}$ selectivity at 30 bar constant pressure, WHSV = 1 h^{-1}, time elapsed: 8 h; Rate of H_2 flow =3600 mL h^{-1}

S. no.	Temperature	<Cn_4	<Cn_{14}	Cn_{15}	Cn_{16}	Cn_{17}	Cn_{18}
1	300	6.4	11.2	24.5	30.3	14	20.1
2	325	6.6	10.5	24.6	27.5	14.8	22.6
3	350	4.6	10.1	17.8	26.8	15.4	29.9
4	375	3.2	13.3	12.6	28.1	21.2	24.5

Table 3. Influence of WHSV at 30 bar constant pressure, precursor: 7% castor oil, WHSV = 1h^{-1}, time elapsed: 5 h; rate of H_2 flow = 3600 mL h−1

S. no.	WHSV(h^{-1})	<Cn_4	<Cn_{14}	Cn_{15}	Cn_{16}	Cn_{17}	Cn_{18}
1	0.5	2.5	5.1	21.4	25.8	17.3	30.7
2	1.0	3.1	7.9	22.6	24.7	16.8	28.8
3	1.5	5.5	14.1	22.4	24.5	18.1	20.2
4	2.0	8.5	20.3	24.6	24.1	16.2	14.2

Time on Stream (TOS)

The evolution of selectivity for the MZC-A catalyst during the 36-hour conversion of castor oil illustrates the influence of time on stream, as depicted in Fig.5. At the beginning, the castor oil's selectivity over the MZC-A catalyst was roughly 65% within the first hour. For the carbon chains Cn_1–Cn_5, Cn_6–Cn_{13}, Cn_{14}–Cn_{15}, Cn_{16}, Cn_{17}, and Cn_{18}, the selectivity was 7%, 4%, 18%, 30%, 19%, and 22%, in that order. Hydrocarbons in the Cn_1–Cn_{18} range were among the end products. Over time, the catalyst's selectivity output rose and reached its peak after roughly 10 hours. The selectivity, however, was altered to 1.3%, 7.4%, 12.9%, 23.5%, 21.2%, and 28.8% for Cn_1–Cn_5, Cn_6–Cn_{13}, Cn_{14}–Cn_{15}, Cn_{16}, Cn_{17}, and Cn_{18}, respectively. The conversion along with selectivity reached a steady state and showed only slight variations with time-on-stream after the tenth hour.

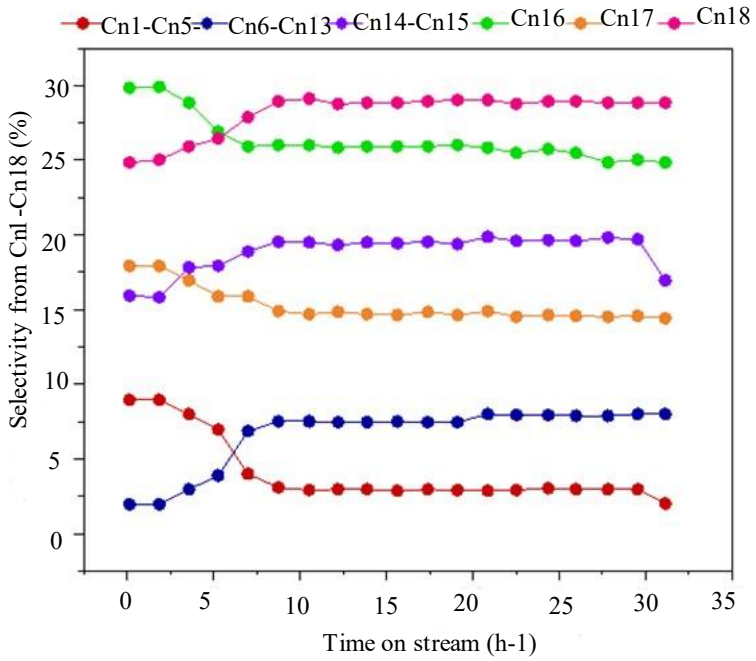

Figure 5. TOS at 30 bar pressure, 350 °C temperature, precursor: 7% castor oil, WHSV = 1 h^{-1}, time elapsed: 8 h; Rate of H2 flow= 3600 mL h^{-1}

CONCLUSION

Various porous matrix catalysts containing Co-Pt metal, including MZC-A, MZC-B and MZC-C (HZSM-5, MCM-41, and H-USY respectively), were synthesized for assessing their HDOx activity on industrial oils. Various metrics including selectivity, stability, conversion rate, turnover frequency (TOF), and SRR (Selectivity to Reaction Rate) were utilized to evaluate the conversion performance of different catalysts. Altering the porous supports markedly influenced the catalytic efficiency of the HDOx reaction, leading to improved textural characteristics. The Co/Pt/HZSM-5 catalyst demonstrated the highest activity of all the tested catalysts. The availability of favourable chemical and physical attributes such as subtle acid centres, ample surface area for H_2 adsorption, and an efficient dissemination of catalytic metals, was linked towards increased catalytic efficiency. During the hydrodeoxygenation of castor oil, the Co/Pt/HZSM-5 catalyst demonstrated superior catalytic activity compared to the other metal-mesoporous supported catalysts. End results showed that the Co/Pt/HZSM-5 catalysts were the most selective for Cn_{1-5}, Cn_{6-13}, Cn_{14-15}, Cn_{16}, Cn_{17}, and Cn_{18}, with corresponding values of 1.3%, 7.4%, 12.9%, 23.5%, 21.2%, and 28.8%. Similarly, for the Co/Pt-HZSM-5 catalyst, the impacts of pressure, temperature, weight hourly space velocity (WHSV), and duration on the stream were examined.

Conflicts of Interest

Nothing to report in terms of conflicts exists.

REFERENCES

1. Arroyo M, Briones L, Hernando H, Escola JM, Serrano DP. Selective decarboxylation of fatty acids catalyzed by Pd-supported hierarchical ZSM-5 zeolite. Energy & Fuels. 2021 Aug 16;35(21):17167-81.
2. Zhang J, Wu Z, Li X, Zhang Y, Bao Z, Bai L, Wang F. Catalytic cracking of inedible oils for the production of drop-in biofuels over a SO42–/TiO2-ZrO2 catalyst. Energy & Fuels. 2020 Oct 21;34(11):14204-14.
3. Zamani AS, Saidi M, Najafabadi AT. Selective production of diesel-like alkanes via Neem seed oil hydrodeoxygenation over Ni/MgSiO3 catalyst. Renewable Energy. 2023 Jun 1;209:462-70.

4. Tsiotsias AI, Hafeez S, Charisiou ND, Al-Salem SM, Manos G, Constantinou A, AlKhoori S, Sebastian V, Hinder SJ, Baker MA, Polychronopoulou K. Selective catalytic deoxygenation of palm oil to produce green diesel over Ni catalysts supported on ZrO2 and CeO2–ZrO2: Experimental and process simulation modelling studies. Renewable energy. 2023 Apr 1;206:582-96.
5. Lucantonio S, Di Giuliano A, Rossi L, Gallucci K. Green diesel production via deoxygenation process: a review. Energies. 2023 Jan 11;16(2):844.
6. Hongloi N, Prapainainar P, Prapainainar C. Review of green diesel production from fatty acid deoxygenation over Ni-based catalysts. Molecular Catalysis. 2022 May 1;523:111696.
7. Chia SR, Nomanbhay S, Ong MY, Chew KW, Show PL. Renewable diesel as fossil fuel substitution in Malaysia: A review. Fuel. 2022 Apr 15;314:123137.
8. Upadhyay PR, Das P. Catalytic Materials for Green Diesel Production. Green Diesel: An Alternative to Biodiesel and Petrodiesel. 2022 May 22:55-108.
9. Azelee NI, da Silva Santos DH, Meili L, Mahdi HI. Commercial Green Diesel Production Under Hydroprocessing Technology Using Solid-Based Heterogeneous Catalysts. InGreen Diesel: An Alternative to Biodiesel and Petrodiesel 2022 May 22 (pp. 149-204). Singapore: Springer Nature Singapore.
10. Ghumman AS, Shamsuddin R, Nasef MM, Krivoborodov EG, Ahmad S, Zanin AA, Mezhuev YO, Abbasi A. A degradable inverse vulcanized copolymer as a coating material for urea produced under optimized conditions. Polymers. 2021 Nov 22;13(22):4040.
11. Lin JK, Lee CP, Lin HP, Halim E, Wang WC. The production of hydro-processed renewable diesel over the nonsulfide catalyst. International Journal of Energy Research. 2021 Oct 25;45(13):19043-61.
12. Mahdi HI, Bazargan A, McKay G, Azelee NI, Meili L. Catalytic deoxygenation of palm oil and its residue in green diesel production: A current technological review. Chemical Engineering Research and Design. 2021 Oct 1;174:158-87.
13. Zhou G, Zhao S, Xie F, Chen S, Xie H. Construction of surface active centers on the mesoporous Co/CeO2-δ catalysts for CO2 hydrogenation. International Journal of Hydrogen Energy. 2023 Aug 29;48(74):28980-97.
14. Yan P, Kennedy E, Stockenhuber M. Natural zeolite supported Ni catalysts for hydrodeoxygenation of anisole. Green Chemistry. 2021;23(13):4673-84.
15. Ranjbar A, Aghamiri SF, Irankhah A. Effect of MgO/Al2O3 ratio in the support of mesoporous Ni/MgO–Al2O3 catalysts for CO2 utilization via reverse water gas shift reaction. International Journal of Hydrogen Energy. 2023 Jun 12;48(50):19115-25.
16. Wu K, Chen F, Wang F, Huang Y, Shen Z, Wang W, Yang Y. Preparation of Pt supported on mesoporous Mg–Al oxide catalysts for efficient dehydrogenation of methylcyclohexane. International Journal of Hydrogen Energy. 2021 Jul 21;46(50):25513-9.
17. Li T, Cheng J, Zhang X, Liu J, Huang R, Zhou J. Jet range hydrocarbons converted from microalgal biodiesel over mesoporous zeolite-based catalysts. International Journal of Hydrogen Energy. 2018 May 24;43(21):9988-93.
18. Cheng J, Zhang Z, Zhang X, Fan Z, Liu J, Zhou J. Continuous hydroprocessing of microalgae biodiesel to jet fuel range hydrocarbons promoted by Ni/hierarchical mesoporous Y zeolite catalyst. International journal of hydrogen energy. 2019 May 3;44(23):11765-73.
19. Kozhukhova AE, du Preez SP, Bessarabov DG. Development of Pt–Co/Al2O3 bimetallic catalyst and its evaluation in catalytic hydrogen combustion reaction. International Journal of Hydrogen Energy. 2024 Jan 2;51:1079-96.
20. Wei Y, Yang W, Yang Z. An excellent universal catalyst support-mesoporous silica: Preparation, modification and applications in energy-related reactions. International Journal of Hydrogen Energy. 2022 Feb 22;47(16):9537-65.
21. Yan P, Bryant G, Li MM, Mensah J, Kennedy E, Stockenhuber M. Shape selectivity of zeolite catalysts for the hydrodeoxygenation of biocrude oil and its model compounds. Microporous and Mesoporous Materials. 2020 Dec 15;309:110561.

22. Cho KH, Chakraborty D, Cho EB, Jung SY, Han H. Newly design and synthesis of Ni–Ir–Ru-doped mesoporous silica open-frameworks for admirable electrochemical water-oxidation application. International Journal of Hydrogen Energy. 2024 Jan 2;51:733-47.
23. Naji SZ, Tye CT, Abd AA. State of the art of vegetable oil transformation into biofuels using catalytic cracking technology: Recent trends and future perspectives. Process Biochemistry. 2021 Oct 1;109:148-68.
24. Loy AC, Alhazmi H, Lock SS, Yiin CL, Cheah KW, Chin BL, How BS, Yusup S. Life-cycle assessment of hydrogen production via catalytic gasification of wheat straw in the presence of straw derived biochar catalyst. Bioresource technology. 2021 Dec 1;341:125796.
25. Arefi-Oskoui S, Khataee A, Ucun OK, Kobya M, Hanci TÖ, Arslan-Alaton I. Toxicity evaluation of bulk and nanosheet MoS2 catalysts using battery bioassays. Chemosphere. 2021 Apr 1;268:128822.
26. Ghumman AS, Shamsuddin R, Nasef MM, Yahya WZ, Abbasi A. Optimization of synthesis of inverse vulcanized copolymers from rubber seed oil using response surface methodology. Polymer. 2021 Mar 26;219:123553.
27. Jing Han S, Ameen M, Hanifah MF, Aqsha A, Bilad MR, Jaafar J, Kheawhom S. Catalytic evaluation of nanoflower structured manganese oxide electrocatalyst for oxygen reduction in alkaline media. Catalysts. 2020 Jul 23;10(8):822.
28. Yang R, Du X, Zhang X, Xin H, Zhou K, Li D, Hu C. Transformation of jatropha oil into high-quality biofuel over Ni–W bimetallic catalysts. ACS omega. 2019 Jun 18;4(6):10580-92.
29. Tsiotsias AI, Hafeez S, Charisiou ND, Al-Salem SM, Manos G, Constantinou A, AlKhoori S, Sebastian V, Hinder SJ, Baker MA, Polychronopoulou K. Selective catalytic deoxygenation of palm oil to produce green diesel over Ni catalysts supported on ZrO2 and CeO2–ZrO2: Experimental and process simulation modelling studies. Renewable energy. 2023 Apr 1;206:582-96.
30. Lin D, Mao Z, Feng X, Zhou X, Yan H, Zhu H, Liu Y, Chen X, Tuo Y, Peng C, Chen D. Kinetic insights into deoxygenation of vegetable oils to produce second-generation biodiesel. Fuel. 2023 Feb 1;333:126416.
31. Pal N, Verma V, Khan A, Mishra A, Anand M, Pramod CV, Farooqui SA, Sinha AK. Hydrotreating and hydrodemetalation of raw jatropha oil using mesoporous Ni-Mo/γ-Al2O3 catalyst. Fuel. 2022 Oct 15;326:125108.
32. Kaewtrakulchai N, Fuji M, Eiad-Ua A. Catalytic deoxygenation of palm oil over metal phosphides supported on palm fiber waste derived activated biochar for producing green diesel fuel. RSC advances. 2022;12(40):26051-69.
33. Yan P, Li MM, Kennedy E, Adesina A, Zhao G, Setiawan A, Stockenhuber M. The role of acid and metal sites in hydrodeoxygenation of guaiacol over Ni/Beta catalysts. Catalysis Science & Technology. 2020;10(3):810-25.
34. Berenguer A, Sankaranarayanan TM, Gómez G, Moreno I, Coronado JM, Pizarro P, Serrano DP. Evaluation of transition metal phosphides supported on ordered mesoporous materials as catalysts for phenol hydrodeoxygenation. Green chemistry. 2016;18(7):1938-51.
35. Song W, Zhao C, Lercher JA. Importance of size and distribution of Ni nanoparticles for the hydrodeoxygenation of microalgae oil. Chemistry–A European Journal. 2013 Jul 22;19(30):9833-42.
36. Fatsikostas AN, Verykios XE. Reaction network of steam reforming of ethanol over Ni-based catalysts. Journal of catalysis. 2004 Jul 25;225(2):439-52.
37. Lei X, Du X, Xin H, Chen X, Yang H, Zhou L, Zeng Y, Zhang H, Tian Y, Li D, Hu C. Chemical-switching strategy for the production of green biofuel on NiCo/MCM-41 catalysts by tuning atmosphere. Fuel. 2022 May 1;315:123118.
38. Fu L, Ba W, Li Y, Li X, Zhao J, Zhang S, Liu Y. Hydrodeoxygenation of non-edible bio-lipids to renewable hydrocarbons over mesoporous SiO2-TiO2 supported NiMo bimetallic catalyst. Applied Catalysis A: General. 2022 Mar 5;633:118475.

39. Soni VK, Dhara S, Krishnapriya R, Choudhary G, Sharma PR, Sharma RK. Highly selective Co3O4/silica-alumina catalytic system for deoxygenation of triglyceride-based feedstock. Fuel. 2020 Apr 15;266:117065.
40. Perumal T, Mangesh VL, Perumal SK, Arumugam R, Subramanian N, Subramanian S, Kannan S. Isomerization of alkanes over ionic liquids supported on SBA-15. Energy & Fuels. 2020 Sep 28;34(11):14620-32.
41. Mangesh VL, Tamizhdurai P, Umasankar S, Palaniswamy R, Narayanan S, Augustine T, Kumaran R, ALOthman ZA, Ouladsmane M, Govindasamy M. Hydroprocessing mixed waste plastics to obtain clean transport fuel. Journal of Cleaner Production. 2022 Jul 15;358:131952.
42. Tamizhdurai P, Sakthinathan S, Krishnan PS, Ramesh A, Mangesh VL, Abilarasu A, Narayanan S, Shanthi K, Chiu TW. Catalytic activity of ratio-dependent SBA-15 supported zirconia catalysts for highly selective oxidation of benzyl alcohol to benzaldehyde and environmental pollutant heavy metal ions detection. Journal of Molecular Structure. 2019 Jan 15;1176:650-61.
43. Tamizhdurai P, Ramesh A, Krishnan PS, Mangesh VL, Umasankar S, Narayanan S, Ragupathi C, Shanthi K. Hydrogenation of dicyclopentadiene into endo-tetrahydrodicyclopentadie over supported different metal catalysts. Microporous and Mesoporous Materials. 2019 Dec 1;290:109678.
44. Ali MA, Brisdon B, Thomas WJ. Synthesis, characterization and catalytic activity of ZSM-5 zeolites having variable silicon-to-aluminum ratios. Applied Catalysis A: General. 2003 Oct 8;252(1):149-62.
45. Kumar D, Schumacher K, von Hohenesche CD, Grün M, Unger KK. MCM-41, MCM-48 and related mesoporous adsorbents: their synthesis and characterisation. Colloids and Surfaces A: Physicochemical and Engineering Aspects. 2001 Aug 31;187:109-16.
46. Ramesh A, Tamizhdurai P, Mangesh VL, Palanichamy K, Gopinath S, Sureshkumar K, Shanthi K. Mg/SiO2–Al2O3 supported nickel catalysts for the production of naphthenic hydrocarbon fuel by hydro-de-oxygenation of eugenol. International Journal of Hydrogen Energy. 2019 Oct 4;44(47):25607-20.
47. Sonthalia A, Kumar N. Comparison of fuel characteristics of hydrotreated waste cooking oil with its biodiesel and fossil diesel. Environmental Science and Pollution Research. 2021 Mar;28(10):11824-34.
48. Fazli-Ku MS, Tye CT. Catalytic Cracking of Waste Cooking Oil Over Activated Carbon Supported Trimetallic Oxide Catalysts. Available at SSRN 4739707.
49. Abdulkareem-Alsultan G, Asikin-Mijan N, Mustafa-Alsultan G, Lee HV, Wilson K, Taufiq-Yap YH. Efficient deoxygenation of waste cooking oil over Co 3 O 4–La 2 O 3-doped activated carbon for the production of diesel-like fuel. RSC advances. 2020;10(9):4996-5009.
50. Janampelli S, Darbha S. Promotional Effect of WOx in Pt-WOx/AlPO4-5 Catalyzed Deoxygenation of Fatty Acids. ChemistrySelect. 2017 Feb 13;2(5):1895-901.
51. Hanafi SA, Elmelawy MS, Shalaby NH, El-Syed HA, Eshaq G, Mostafa MS. Hydrocracking of waste chicken fat as a cost effective feedstock for renewable fuel production: A kinetic study. Egyptian Journal of Petroleum. 2016 Dec 1;25(4):531-7.
52. Phimsen S, Kiatkittipong W, Yamada H, Tagawa T, Kiatkittipong K, Laosiripojana N, Assabumrungrat S. Oil extracted from spent coffee grounds for bio-hydrotreated diesel production. Energy Conversion and Management. 2016 Oct 15;126:1028-36.

